

000 001 002 003 004 005 006 007 008 009 010 011 012 013 014 015 016 017 018 019 020 021 022 023 024 025 026 027 028 029 030 031 032 033 034 035 036 037 038 039 040 041 042 043 044 045 046 047 048 049 050 051 052 053 ALITA-G: SELF-EVOLVING GENERATIVE AGENT FOR AGENT GENERATION

Anonymous authors

Paper under double-blind review

ABSTRACT

Large language models (LLMs) perform better when scaffolded into agents with memory, tools, and feedback. Beyond this, self-evolving agents have emerged, but current work largely limits adaptation to prompt rewriting or failure retries. Therefore, we present ALITA-G, a self-evolution framework that transforms a general-purpose agent into a domain expert by systematically generating, abstracting, and curating Model Context Protocol (MCP) tools. In this framework, a generalist agent executes a curated suite of target-domain tasks and synthesizes candidate MCPs from successful trajectories. These are then abstracted to parameterized primitives and consolidated into a *MCP Box*. At inference time, ALITA-G performs retrieval-augmented MCP selection with the help of each tool’s descriptions and use cases, before executing an agent equipped with the MCP Executor. Across several benchmarks GAIA, PathVQA, and Humanity’s Last Exam, ALITA-G attains strong gains while reducing computation costs. On GAIA validation, it achieves 83.03% pass@1 and 89.09% pass@3, establishing a new state-of-the-art result while reducing mean tokens per example by approximately 15% relative to a strong baseline agent. ALITA-G thus provides a principled pathway from generalist capability to reusable, domain-specific competence, improving both accuracy and efficiency on complex reasoning tasks.

1 INTRODUCTION

Large language models (LLMs) have demonstrated strong performance across a wide range of tasks [1; 2]. However, a standalone LLM is still often insufficient for complex real-world tasks, especially those that demand professional domain knowledge and difficult multi-step reasoning. To further enhance their problem-solving capability, recent work constructs agentic systems around LLMs that decompose tasks, orchestrate tools and data sources, and iterate via feedback [3; 4; 5]. Embedding an LLM within an agentic system mitigates the limitations of its parametric knowledge and, by leveraging external knowledge sources and tools, enables deep research ability, demonstrating remarkable capabilities in task decomposition, tool coordination, and adaptive reasoning across diverse domains [6; 7]. Beyond these abilities, a distinguishing property of advanced agent systems is their potential for self-evolution [2; 8]: by leveraging self-generated content and both internal and external feedback, they can bootstrap their capabilities and, with minimal explicit human intervention, evolve into increasingly capable agent systems.

Despite rapid progress in self-evolving agents, current systems still exhibit limitations that constrain their evolutionary potential and downstream performance. Evolution is often narrow in scope: agents iteratively polish performance in a single target task or a restricted domain without the capacity to lift a general-purpose agent into a domain expert across a set of related tasks [4; 9]. At the same time, evolution is typically shallow in mechanism: many methods tune only a limited subset of modules or tools [10; 11], or a or rely on error-repair heuristics [12], instead of performing task-conditioned, end-to-end adaptation of the whole architecture. End-to-end evolution is important since real tasks demand planning, decomposition, tool use, and memory to improve together rather than in isolation. Likewise, transforming a general agent into a domain expert across a task set improves transfer and sample efficiency within that domain, supports robust generalization to new but related tasks, and sustains long-horizon improvement.

To address these limitations, we define a new paradigm of self-evolution: transforming a general-purpose agent into a domain expert across a set of tasks through task-conditioned, end-to-end adaptation. Building on this paradigm, we introduce ALITA-G, a framework that enables such transformation and achieves substantially improved performance within the target domain. to deep expertise and strong performance on domain-specific tasks. Our method employs a multi-execution strategy, where a generalist agent repeatedly engages the task collection and systematically synthesizes diverse Model Context Protocol (MCP) [13] components to capture, generalize, and adapt behaviors across executions. Across iterations, we harvest high-quality MCPs from successful runs and subject them to abstraction and refinement to build domain-specific MCP repositories, referred to as *MCP Box*. These repositories serve as specialized toolkits that support retrieval-augmented tool selection at inference time, allowing agents to dynamically identify and invoke the most contextually relevant MCPs for novel tasks in their specialization domain. From a system-level perspective, ALITA-G integrates two central dimensions. It is evolving as it end-to-end transforms a general agent into a domain specialist, and it is generative as it instantiates task-specific specialists on demand. This dual capability improves both the efficiency of agent construction and the effectiveness of domain problem solving.

We conduct comprehensive experiments across diverse benchmarks, GAIA [14], PathVQA [15], and Humanity’s Last Exam [16], to validate the effectiveness of our approach. The results demonstrate that ALITA-G generates high-performing domain-specialist agents across multiple domains: these specialists deliver strong in-domain performance while reducing computational overhead relative to a generalist agent. On the challenging GAIA benchmark, our method achieves 83.03% pass@1 and 89.09% pass@3 accuracy, establishing a new state-of-the-art performance. Detailed ablations and analyses confirmed the necessity of each component and the advantages of our key hyperparameter choices. Our contribution can be summarized in three dimensions:

- We present ALITA-G, a novel self-evolution framework that transforms generalist agents into domain specialists to achieve substantially improved performance within a specific domain.
- We are the first to couple MCP abstraction with MCP-level retrieval-augmented generation (RAG) in a single framework. This design distills task-specific MCPs into reusable primitives and retrieves them at inference, yielding consistent gains in accuracy while reducing compute and latency.
- Across diverse benchmarks, our method improves performance while reducing compute; on the GAIA validation set, it achieves 83.03% pass@1 and 89.09% pass@3 (new SOTA), scales with MCP Box richness, and ablations verify the contribution of each component.

2 METHODS

We introduce ALITA-G, a novel framework for automatic agent generation that constructs task-specific agents through systematic MCP box curation and retrieval-augmented tool selection. Our approach addresses the fundamental challenge of agent design automation by leveraging task-driven MCP generation and intelligent tool filtering mechanisms, overcoming the limitations of prior methods that are narrow in scope or shallow in mechanism.

2.1 PROBLEM FORMULATION

Given a collection of target tasks $\mathcal{T} = \{(x_i, y_i)\}_{i=1}^N$ where x_i represents task specifications and y_i denotes desired outcomes, our objective is to automatically synthesize a specialized agent $\pi_{\text{specialized}}$ capable of effectively handling tasks within the domain defined by \mathcal{T} .

Formally, we aim to construct:

$$\pi_{\text{specialized}} = \text{Alita-G}(\mathcal{T}, \pi_{\text{master}}), \quad (1)$$

where π_{master} is a powerful general-purpose agent system, and the resulting specialized agent should satisfy:

$$\mathbb{E}_{(x,y) \sim \mathcal{D}_{\text{target}}} [\mathbb{I}\{\pi_{\text{specialized}}(x) = y\}] > \mathbb{E}_{(x,y) \sim \mathcal{D}_{\text{target}}} [\mathbb{I}\{\pi_{\text{base}}(x) = y\}], \quad (2)$$

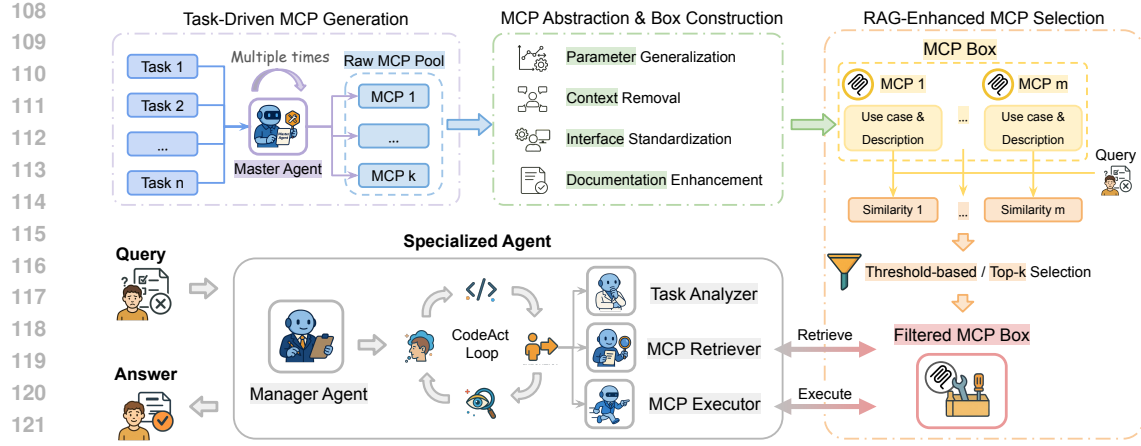


Figure 1: Overall workflow of ALITA-G. The process begins with task-driven MCP generation, where a Master Agent repeatedly executes target tasks and distills a pool of raw MCPs from successful trajectories. These MCPs are then abstracted and refined through parameter generalization, context removal, interface standardization, and documentation enhancement to form a reusable *MCP Box*. At inference time, the MCP Box supports RAG-enhanced tool selection: user queries are matched against MCP descriptions, and threshold/top- k filtering yields a contextually relevant set of MCPs. Finally, a specialized agent—comprising a Manager Agent with a Task Analyzer, MCP Retriever, and MCP Executor—runs a CodeAct loop to retrieve and invoke the selected MCPs, thereby transforming a general-purpose agent into a domain specialist for end-to-end task solving.

where $\mathcal{D}_{\text{target}}$ represents the target task distribution and π_{base} denotes a baseline agent without specialized capabilities.

2.2 TASK-DRIVEN MCP GENERATION

Our framework begins with systematic MCP generation through the master agent’s task execution. When processing each task $(x_i, y_i) \in \mathcal{T}$, the master agent π_{master} produces a reasoning trajectory:

$$\tau_i = (r_1^{(i)}, a_1^{(i)}, o_1^{(i)}, \dots, r_{L_i}^{(i)}, a_{L_i}^{(i)}, o_{L_i}^{(i)}), \quad (3)$$

where $r_t^{(i)} \in \mathcal{R}$ represents reasoning tokens, $a_t^{(i)} \in \mathcal{A}$ denotes action tokens (including MCP generation calls), and $o_t^{(i)} \in \mathcal{O}$ corresponds to environmental observations.

During trajectory execution, the master agent is guided by explicit prompting to externalize reusable sub-solutions as self-contained MCPs rather than only producing final answers. The prompt instructs the agent to modularize complex sub-tasks into callable procedures with standardized interfaces and documentation, so that solving a task also expands the MCP pool for future reuse. We denote the j -th MCP generated during the execution of task i as $\text{MCP}_{i,j}$, which includes both the executable code and associated metadata:

$$\text{MCP}_{i,j} = \{\text{code}_{i,j}, \text{description}_{i,j}, \text{use_case}_{i,j}\}, \quad (4)$$

where $\text{description}_{i,j}$ provides a concise functional summary and $\text{use_case}_{i,j}$ records the specific task context that triggered the MCP’s creation.

To ensure quality and reliability, we implement a multi-execution strategy where each task (x_i, y_i) is executed K times, generating potentially different MCP variants. We collect MCPs only from successful executions where $\pi_{\text{master}}(x_i) = y_i$, forming the raw MCP pool:

$$\mathcal{L} = \{\text{MCP}_{i,j}^{(k)} \mid \pi_{\text{master}}^{(k)}(x_i) = y_i, i \in [N], j \in [J_{k,i}], k \in [K]\}, \quad (5)$$

162 where $J_{k,i}$ denotes the number of MCPs generated for task i during the k -th execution run.
 163

164 **2.3 MCP ABSTRACTION AND BOX CONSTRUCTION**
 165

166 Following the principles established in agent distillation literature, we apply abstraction techniques
 167 to transform instance-specific MCPs into generalizable tools. For each MCP in the raw pool \mathcal{L} , we
 168 employ a high-capacity language model to perform abstraction:
 169

$$170 \quad \widehat{\text{MCP}}_{i,j}^{(k)} = \text{LLM}_{\text{abstract}}(\text{MCP}_{i,j}^{(k)}) \quad (6)$$

172 The abstraction process accomplishes several critical transformations:
 173

- 174 • **Parameter Generalization:** Replace hard-coded values with configurable parameters
- 175 • **Context Removal:** Eliminate task-specific references while preserving core functionality
- 176 • **Interface Standardization:** Ensure compatibility with FastMCP [17] protocol specifications,
 177 which is a high-performance implementation of the Model Context Protocol that
 178 provides optimized runtime support for dynamic tool integration and execution.
- 179 • **Documentation Enhancement:** Generate comprehensive docstrings and type annotations

181 Unlike traditional clustering approaches, our method preserves the diversity of MCP implementations
 182 to maximize coverage of potential task variations. The complete MCP box is defined as:
 183

$$184 \quad \mathcal{B} = \{\widehat{\text{MCP}}_m \mid m \in [M]\}, \quad (7)$$

186 where $M = |\mathcal{L}|$ represents the total number of abstracted MCPs, and each $\widehat{\text{MCP}}_m$ maintains its
 187 original metadata structure with abstracted code, preserved description, and use case information.
 188

189 **2.4 RAG-ENHANCED MCP SELECTION**
 190

191 To address the challenge of tool relevance in diverse task scenarios, we introduce a retrieval-augmented
 192 generation mechanism for dynamic MCP selection. For each $\widehat{\text{MCP}}_m \in \mathcal{B}$, we construct a composite
 193 representation by concatenating its description and use case: $\text{context}_m = \text{description}_m \oplus \text{use_case}_m$,
 194 where \oplus denotes string concatenation.
 195

196 Given a new task query x_{new} , we compute semantic embeddings for both the query and all MCP
 197 contexts using a pre-trained embedding model ϕ :
 198

$$199 \quad \mathbf{e}_{\text{query}} = \phi(x_{\text{new}}), \mathbf{e}_m = \phi(\text{context}_m), \quad \forall m \in [M] \quad (8)$$

201 The relevance score between the query and each MCP is computed using cosine similarity:
 202

$$203 \quad s_m = \frac{\mathbf{e}_{\text{query}} \cdot \mathbf{e}_m}{\|\mathbf{e}_{\text{query}}\|_2 \|\mathbf{e}_m\|_2} \quad (9)$$

205 Our framework supports two complementary strategies for MCP selection based on the computed
 206 relevance scores:
 207

208 **Threshold-based Selection:** We select MCPs whose relevance scores exceed a predefined threshold
 209 τ :

$$210 \quad \mathcal{B}_{\text{filtered}}^{\text{thresh}} = \{\widehat{\text{MCP}}_m \mid s_m \geq \tau, m \in [M]\} \quad (10)$$

212 This approach ensures that only sufficiently relevant tools are included, providing quality control over
 213 the selected MCP subset while maintaining flexibility in the number of selected tools.

214 **Top-k Selection:** Alternatively, we select the k MCPs with the highest relevance scores:
 215

$$216 \quad \mathcal{B}_{\text{filtered}}^{\text{top-k}} = \{\widehat{\text{MCP}}_m \mid m \in \text{argsort}(\{s_j\}_{j=1}^M)[-k :]\} \quad (11)$$

216 This strategy guarantees a fixed number of tools for consistent computational overhead while ensuring
 217 that the most relevant MCPs are always selected, regardless of their absolute similarity scores.
 218

219 The choice between threshold-based and top-k selection depends on task characteristics and computa-
 220 tional constraints. Threshold-based selection adapts the tool set size to task complexity, while top-k
 221 selection provides predictable resource utilization. This RAG-based filtering mechanism ensures
 222 that the specialized agent operates with a focused, relevant tool set for each specific task, thereby
 223 improving both efficiency and performance.
 224

225 2.5 SPECIALIZED AGENT ARCHITECTURE

226 The final specialized agent $\pi_{\text{specialized}}$ integrates the master agent’s core reasoning capabilities together
 227 with the curated MCP box and RAG-based tool selection mechanism. The agent architecture
 228 comprises:
 229

- 230 • **Task Analyzer:** Processes incoming tasks and generates appropriate embedding representa-
 231 tions
- 232 • **MCP Retriever:** Implements the RAG-based selection algorithm to identify relevant tools
- 233 • **MCP Executor:** Provides runtime support for dynamic tool invocation with standardized
 234 interfaces

235 The inference process follows a structured pipeline that accommodates both selection strategies. A
 236 detailed workflow is shown in Algorithm algorithm 1.
 237

238 Through this systematic approach, ALITA-G automatically constructs specialized agents that inherit
 239 the master agent’s reasoning capabilities while being equipped with task-specific, efficiently retriev-
 240 able tools, thereby achieving superior performance on target task domains with minimal manual
 241 intervention.
 242

243 3 EXPERIMENTS

245 Through extensive experiments on diverse task domains, we demonstrate that ALITA-G produces
 246 automatically generated agents that consistently surpass general-purpose agents in both accuracy and
 247 efficiency.
 248

249 3.1 EXPERIMENTAL SETUP

251 **Settings.** Throughout all experiments, we employ a unified agent architecture consisting of a
 252 Manager Agent and a Web Agent, following the Alita framework [4]. The Manager Agent utilizes
 253 Claude-Sonnet-4 as the base model for high-level task coordination and reasoning, while the Web
 254 Agent leverages GPT-4.1 for external information retrieval and web interactions. We select the
 255 currently most powerful text embedding model, OpenAI’s text-embedding-3-large [18], as the
 256 embedding computation model, and employ threshold mode for filtering, incorporating MCPs with
 257 similarity scores greater than $\tau = 0.7$ for usage. We use GAIA [14], PathVQA [15] and The
 258 Humanity’s Last Exam (HLE) [16] as benchmarks, details can be found in Appendix C. We report
 259 both the accuracy achieved on these benchmarks and the average number of tokens consumed during
 260 answer generation.
 261

262 **Baselines.** We compare our approach against several state-of-the-art agent systems and variants of
 263 our method:
 264

- 265 • **Octotools** [19]: A tool-augmented agent framework that provides agents with access to a
 266 predefined collection of specialized tools for various tasks.
- 267 • **ODR-smolagents** [20]: The Open Deep Research agent implementation within the Smola-
 268 gents framework, representing a strong baseline for general-purpose agent capabilities.
- 269 • **Original Agent System:** The master agent used for MCP generation, evaluated without
 270 access to the specialized MCP box to establish the baseline performance of the underlying
 271 architecture.

Method	Metric	GAIA				PathVQA	HLE
		Level 1	Level 2	Level 3	Total		
<i>Baseline Methods</i>							
Octotools	Accuracy (%)	-	-	-	18.04	47	-
	Avg. Tokens	-	-	-	-	-	-
ODR-smolagents	Accuracy (%)	67.92	53.49	34.62	55.15	42	-
	Avg. Tokens	-	-	-	-	-	-
<i>Original Agent System</i>							
Original (pass@1)	Accuracy (%)	77.36	76.74	65.38	75.15	52	24
	Avg. Tokens	11058	12467	14308	12305	12542	14730
Original (pass@3)	Accuracy (%)	88.68	89.53	76.92	87.27	63	39
	Avg. Tokens	10947	12492	14489	12310	12627	14503
<i>Generated Agents (Our Method)</i>							
ALITA-G ^{1×} (pass@1)	Accuracy (%)	84.91	80.23	69.23	80.00	56	28
	Avg. Tokens	10149	11357	13094	11243	10867	13128
ALITA-G ^{1×} (pass@3)	Accuracy (%)	90.56	89.53	80.77	88.48	64	41
	Avg. Tokens	10259	11297	13027	11236	10862	13096
ALITA-G ^{3×} (pass@1)	Accuracy (%)	86.80	83.72	73.08	83.03	60	33
	Avg. Tokens	9951	10258	11746	10394	10574	11956
ALITA-G ^{3×} (pass@3)	Accuracy (%)	90.56	90.70	80.77	89.09	66	42
	Avg. Tokens	10025	10367	11689	10465	10479	12002

Table 1: Performance comparison across benchmarks and baseline methods. Each method is evaluated on both test accuracy and computational efficiency (measured by average token consumption). **Original** refers to the master agent system used to generate MCP boxes for specialized agents. ALITA-G^{1×} and ALITA-G^{3×} represent our method equipped with MCP boxes generated from single and triple task executions respectively. pass@1 and pass@3 indicate single-attempt and best-of-three-attempts evaluation protocols. Bold values indicate the best performance in each category.

3.2 EXPERIMENTAL RESULTS

Table 1 presents the comprehensive evaluation results across all benchmarks and baseline configurations.

Our experimental results demonstrate several key findings that validate the effectiveness of the proposed ALITA-G framework:

Superior Task-Specific Performance. The automatically generated agents consistently outperform both general-purpose baselines and the original agent system across all benchmarks. ALITA-G (3×) pass@1 achieves 83.03% accuracy on GAIA, representing a 50.5% relative improvement over ODR-smolagents (55.15%) and a 10.3% improvement over the original agent system with pass@1 (75.15%). Similar performance gains between ALITA-G (3×) pass@1 and original agent system pass@1 are observed on PathVQA (60% vs. 52%) and HLE (33% vs. 24%), demonstrating the generalizability of our approach across diverse task domains.

MCP Box Quality Correlation. The comparison between single-generation and triple-generation MCP boxes reveals a clear correlation between MCP box richness and agent performance. The triple-generation variant consistently achieves higher accuracy across all benchmarks, with notable improvements on GAIA (83.03% vs. 80.00%) and more substantial gains on complex reasoning tasks in PathVQA and HLE. This finding supports our hypothesis that multiple execution rounds lead to more comprehensive and robust tool collections.

Computational Efficiency Gains. Remarkably, our specialized agents achieve superior accuracy while demonstrating significantly improved computational efficiency. ALITA-G (3×) reduces average token consumption to 10,394 on GAIA compared to 12,305 for the original baseline, representing a 15.5% efficiency improvement. This dual benefit of enhanced performance and reduced computational cost stems from the targeted nature of the MCP box, which provides agents with precisely the tools needed for specific task categories, eliminating extensive tool search processes.

324 325 326 327 328 329 330	Iter.	Level 1	Level 2	Level 3	Average	# MCPs	# Clusters	Mean Sim.	Median Sim.
	1	84.91	80.23	69.23	80.00	26	26	0.28	0.27
	2	84.91	81.40	71.15	81.82	46	41	0.31	0.29
	3	86.79	82.56	73.08	83.03	74	52	0.30	0.28
	4	86.79	82.56	73.08	83.03	102	60	0.32	0.30
	5	86.79	83.72	73.08	83.63	128	65	0.34	0.31

331
332
333
334
335
336
337
338
339
340
341
342
343
344
345
346
347
348
349
350
351
352
353
354
355
356
357
358
359
360
361
362
363
364
365
366
367
368
369
370
371
372
373
374
375
376
377

Table 2: Performance and MCP Box statistics versus the number of generation iterations k on the GAIA validation set. Accuracies are reported in % for each difficulty level and their average. # MCPs is the count of curated MCPs in the MCP Box after filtering and abstraction. **Mean/Median Sim.** mean statistics of pairwise cosine similarity between MCP embeddings, where Mean Sim. denotes the average pairwise similarity, Median Sim. denotes the Median of pairwise similarities. # Clusters is the number of connected components when linking MCP pairs with similarity (≥ 0.7 , serving as a proxy for the number of independent MCPs. Iter. denotes how many times the original task set is run when constructing the MCP Box.

The consistent improvements across multiple evaluation dimensions provide strong empirical evidence for the effectiveness of our automatic agent generation methodology. These results demonstrate that task-driven MCP curation, combined with intelligent retrieval mechanisms, enables the creation of specialized agents that surpass general-purpose systems in both performance and computational efficiency.

4 ANALYSIS

4.1 ANALYSIS OF MCP BOX SCALABILITY

To understand the performance boundaries of MCP Box expansion and identify the optimal number of generation iterations, we investigate the relationship between MCP generation frequency and agent performance improvements across different task complexities.

Settings. We use the full GAIA validation set and vary the number of *generation iterations* $k \in \{1, 2, 3, 4, 5\}$. Each iteration runs the master agent once over the entire validation set to harvest additional MCPs, followed by filtering and abstraction to construct the accumulated MCP Box. For each k we report: (i) the number of curated MCPs; (ii) summary statistics (mean and median) of pairwise MCP similarity; and (iii) the number of clusters under a fixed similarity threshold. Concretely, we embed each MCP by concatenating its *description* and *use-case* fields, encoding the resulting text with `text-embedding-3-large`, and ℓ_2 -normalizing the embedding. Cosine similarity between two MCPs is then the inner product of their normalized embeddings. To quantify redundancy, we build an undirected similarity graph whose vertices are MCPs and whose edges connect pairs with similarity at least $\tau = 0.7$; the reported cluster count is the number of connected components in this graph. Downstream agent performance is evaluated with the accumulated MCP Box while keeping all other configurations identical to Section 3.

Results. Performance shows substantial gains from iterations 1 to 3 before exhibiting clear saturation and diminishing returns. Table 2 exhibits a clear pattern of diminishing returns in MCP Box scalability. The largest gains occur when increasing the number of generations from $k=1$ to $k=3$, with average accuracy rising from 80.00% to 83.03%. We attribute this improvement to the stochasticity of MCP discovery: the master agent does not consistently surface the most useful MCPs in a single pass, and multiple passes enrich coverage of the task distribution. Beyond $k=3$, additional iterations yield marginal benefits—the average remains flat at $k=4$ and nudges to 83.63% at $k=5$. Per-level trends echo this picture: Level 1 saturates by $k=3$ (84.91 \rightarrow 86.79), Level 3 plateaus thereafter (69.23 \rightarrow 73.08), and the modest late-stage gain is concentrated in Level 2 (82.56 at $k=3$ to 83.72 at $k=5$).

Similarity analysis reveals progressive redundancy accumulation that explains the performance plateau. Complementing these performance trends, the similarity and clustering statistics indicate increasing redundancy as the MCP Box grows. Under the fixed threshold $\tau=0.7$, the number of

Metric	1 Generation	2 Generation	3 Generation
Overall accuracy (%)	80.00	81.52	83.03
Wrong→Right # (vs. baseline)	9	12	13
Right→Wrong # (vs. baseline)	1	1	0
Avg. MCP calls per question	1.9	2.2	2.4
Avg. MCP calls per improved questions	2.7	3.0	3.4

Table 3: MCP usage and outcome metrics on the GAIA validation set across MCP Box configurations. 1 Generation, 2 Generation, and 3 Generation refer to MCP Boxes constructed via one, two, and three iterative generation rounds. **Wrong→Right # (vs. baseline)** counts items that the baseline agent (without an MCP Box) answers incorrectly, but the integrated agent answers correctly. **Right→Wrong # (vs. baseline)** counts items that the baseline answers correctly, but the integrated agent answers incorrectly. **Avg. MCP calls per question** is the mean number of calls to any MCP per question over all instances. **Avg. MCP calls per improved question** are the same mean computed only over the Wrong→Right subset.

connected components—our proxy for effective MCP families—increases sublinearly relative to the total number of curated MCPs: clusters grow from 26 to 65 while MCPs grow from 26 to 128. Consequently, the effective-coverage ratio (#Clusters/#MCPs) drops from 1.00 ($k=1$) to 0.51 ($k=5$), and the marginal yield of new, independent clusters per iteration diminishes (+15, +11, +8, +5 from $k=1 \rightarrow 5$). The performance plateau between $k=3$ and $k=4$ coincides with an addition of 28 MCPs but only 8 new clusters alongside a rise in average similarity, suggesting that later iterations predominantly introduce near-duplicates or narrow variants of existing capabilities. Taken together, these results indicate that $k=3$ offers a favorable balance between computational cost and utility—capturing most of the diverse, high-impact MCP families while avoiding the redundancy that characterizes further expansions.

4.2 MCP BEHAVIOR ANALYSIS

To validate that agents indeed gain enhanced capabilities through MCP Box integration, we conduct a detailed analysis of MCP usage patterns in generated agents.

Settings. We analyze MCP usage behavior on the GAIA validation set using agents equipped with MCP Boxes generated through 1, 2, and 3 iterative rounds, denoted as **1/2/3 Generation**. Beyond usage metrics, we additionally report (a) *overall accuracy* after MCP Box integration, (b) the number of questions flipped from wrong to right (*Wrong→Right*) relative to the baseline (no MCP Box), and (c) the number flipped from right to wrong (*Right→Wrong*). All metrics are computed on the same GAIA validation set. We continue to track the average number of MCP calls per question over all instances and specifically for *improved questions* (incorrect under the baseline but correct after integration). An *MCP call* refers to one invocation to any MCP in the connected MCP Box; the same MCP may be called multiple times within a single task.

Results. Table 3 shows a clear trend of increased MCP utilization as the MCP Box becomes more mature. The average number of MCP calls per question rises monotonically from 1.9 to 2.4 when moving from 1 to 3 generations, while the corresponding average on improved questions increases from 2.7 to 3.4. Notably, improved questions consistently elicit substantially more MCP usage than the overall average—about 1.4× more in all configurations ($2.7/1.9 = 1.42$, $3.0/2.2 = 1.36$, $3.4/2.4 = 1.42$). The marginal increments suggest targeted deployment of MCPs on challenging instances: overall usage grows by +0.3 then +0.2 calls, whereas improved-question usage grows by +0.3 then +0.4, indicating that later generations concentrate additional tool use where it is most impactful.

Turning to answer correctness, overall accuracy improves steadily from 80.00% to 83.03% as the number of generations increases from 1 to 3 (a gain of +3.03 points). These gains are driven primarily by Wrong→Right flips (9/12/13), while Right→Wrong flips are rare (1/1/0), yielding net improvements of +8, +11, and +13 respectively. The low incidence of regressions—vanishing

432 by the 3-generation setting—indicates that the method is robust: it rarely converts correct baseline
 433 answers into errors while delivering consistent accuracy gains as the MCP Box is strengthened. Upon
 434 closer examination of the Right→Wrong cases in the 1- and 2-generation settings, we observe that
 435 these involve distinct questions and stem from reasoning errors introduced during agent execution
 436 rather than incorrect MCP usage. These regressions appear attributable to inherent LLM robustness
 437 limitations within the agent system rather than deficiencies introduced by MCP Box integration.

439 5 RELATED WORKS

441 5.1 AUTO GENERATING AGENT

443 Recent advances in automated agent construction have focused on generating agents or agent systems
 444 with varying degrees of automation and scope. AutoAgents [21] pioneers automatic multi-agent
 445 generation by dynamically creating specialized agents. Building on this foundation, AutoGenesis-
 446 Agent [22] introduces self-generating capabilities with lifecycle management for multi-agent systems,
 447 while EvoAgent [23] applies evolutionary algorithms to extend expert agents into multi-agent con-
 448 figurations. MetaGPT [24] incorporates human software development workflows into LLM-based
 449 multi-agent collaboration. More recently, AutoAgent [25] provides a zero-code framework for
 450 creating LLM agents, and Dynamic LLM-Agent Network [26] focuses on automatic agent team
 451 optimization without requiring strong human priors. Our work differs fundamentally by generating
 452 complete, task-specific agents ready for downstream deployment, rather than focusing on isolated
 453 component generation or requiring extensive manual configuration for integration.

454 5.2 SELF-EVOLVING AGENT

456 Self-evolving agents represent a paradigm where AI systems autonomously improve their capabilities
 457 through iterative learning and adaptation. Recent comprehensive surveys [2] categorize these systems
 458 based on their evolution mechanisms, ranging from parametric updates to non-parametric component
 459 optimization. Early foundational work includes Reflexion [27], which introduces verbal reinforcement
 460 learning for language agents through self-reflection and memory-based learning, and ExpeL [28],
 461 which enables agents to gather and learn from experiential data across training tasks autonomously.
 462 More recent advances have explored diverse self-evolution mechanisms such as SAGE [29], Agent-
 463 Pro [30], Gödel Agent [31], RAGEN [32], EvolveSearch [33] and SELF [34]. Our framework can be
 464 conceptualized as a form of agent self-evolution, where agents leverage previously generated tools
 465 from past task executions to enhance performance on similar future tasks, achieving both improved
 466 accuracy and computational efficiency.

467 5.3 MCP

469 Model Context Protocol (MCP) has emerged as a standardized framework for enabling seamless
 470 integration between AI systems and external tools or data sources [35; 36; 37; 38]. Introduced by
 471 Anthropic [13], MCP provides a unified interface that addresses fragmentation challenges in tool
 472 integration for LLM-based agents. Our methodology relies on constructing high-quality MCP boxes
 473 as the foundation for generating specialized agents, where the richness and relevance of the MCP
 474 collection directly correlates with the resulting agent’s task-specific performance. While [39] also
 475 leverages the MCP as a conduit for distilling capabilities across agents, their focus is on curating
 476 strong teacher agents to assist weaker ones. In contrast, our work targets the end-to-end evolution of a
 477 more powerful domain-specialist agent tailored to a specific target domain, moving beyond assistance
 478 to specialization.

479 6 CONCLUSION

482 In this paper, we introduce ALITA-G, a novel self-evolution framework that transforms generalist
 483 agents to domain-specific experts. By organizing task-derived tools into MCP Boxes with RAG, our
 484 approach significantly enhances agent capabilities on specific domain tasks. Future work could further
 485 expand the ways agents perform self-evolution, enabling even greater leaps in agent development
 through collaborative enhancement across multiple dimensions beyond the current framework.

486 7 REPRODUCIBILITY STATEMENT
487488 We will open-source our code and evaluation scripts upon publication. All datasets, model settings
489 are described in the paper, enabling researchers to reproduce all reported experiments and results.
490491 REFERENCES
492

[1] Hongru Wang, Lingzhi Wang, Yiming Du, Liang Chen, Jingyan Zhou, Yufei Wang, and Kam-Fai Wong. A survey of the evolution of language model-based dialogue systems: Data, task and models, 2025.

[2] Huan-ang Gao, Jiayi Geng, Wenyue Hua, Mengkang Hu, Xinzhe Juan, Hongzhang Liu, Shilong Liu, Jiahao Qiu, Xuan Qi, Yiran Wu, et al. A survey of self-evolving agents: On path to artificial super intelligence. *arXiv preprint arXiv:2507.21046*, 2025.

[3] Guangyao Chen, Siwei Dong, Yu Shu, Ge Zhang, Jaward Sesay, Börje F Karlsson, Jie Fu, and Yemin Shi. Autoagents: A framework for automatic agent generation. *arXiv preprint arXiv:2309.17288*, 2023.

[4] Jiahao Qiu, Xuan Qi, Tongcheng Zhang, Xinzhe Juan, Jiacheng Guo, Yifu Lu, Yimin Wang, Zixin Yao, Qihan Ren, Xun Jiang, et al. Alita: Generalist agent enabling scalable agentic reasoning with minimal predefinition and maximal self-evolution. *arXiv preprint arXiv:2505.20286*, 2025.

[5] Jiahao Qiu, Fulian Xiao, Yimin Wang, Yuchen Mao, Yijia Chen, Xinzhe Juan, Shu Zhang, Siran Wang, Xuan Qi, Tongcheng Zhang, et al. On path to multimodal historical reasoning: Histbench and histagent. *arXiv preprint arXiv:2505.20246*, 2025.

[6] Zhiheng Xi, Wenxiang Chen, Xin Guo, Wei He, Yiwen Ding, Boyang Hong, Ming Zhang, Junzhe Wang, Senjie Jin, Enyu Zhou, et al. The rise and potential of large language model based agents: A survey. *arXiv preprint arXiv:2309.07864*, 2023.

[7] Yujia Qin, Shihao Liang, Yining Ye, Kunlun Zhu, Lan Yan, Yaxi Lu, Yankai Lin, Xin Cong, Xiangru Tang, Bill Qian, et al. Tool learning with foundation models. *arXiv preprint arXiv:2304.08354*, 2023.

[8] Jinyuan Fang, Yanwen Peng, Xi Zhang, Yingxu Wang, Xinhao Yi, Guibin Zhang, Yi Xu, Bin Wu, Siwei Liu, Zihao Li, et al. A comprehensive survey of self-evolving ai agents: A new paradigm bridging foundation models and lifelong agentic systems. *arXiv preprint arXiv:2508.07407*, 2025.

[9] Jiabin Tang, Tianyu Fan, and Chao Huang. Autoagent: A fully-automated and zero-code framework for llm agents. *arXiv e-prints*, pages arXiv–2502, 2025.

[10] Yongchao Zhou, Andrei Ioan Muresanu, Ziwen Han, Keiran Paster, Silviu Pitis, Harris Chan, and Jimmy Ba. Large language models are human-level prompt engineers. In *International Conference on Learning Representations*, 2023.

[11] Yujia Qin, Shihao Liang, Yining Ye, Kunlun Zhu, Lan Yan, Yaxi Lu, Yankai Lin, Xin Cong, Xiangru Tang, Bill Qian, et al. Toolllm: Facilitating large language models to master 16000+ real-world apis. *arXiv preprint arXiv:2307.16789*, 2023.

[12] Xiang Huang, Sitao Cheng, Shanshan Huang, Jiayu Shen, Yong Xu, Chaoyun Zhang, and Yuzhong Qu. Queryagent: A reliable and efficient reasoning framework with environmental feedback-based self-correction. *arXiv preprint arXiv:2403.11886*, 2024.

[13] Anthropic. Introducing the model context protocol, 2024.

[14] Grégoire Mialon, Clémentine Fourrier, Thomas Wolf, Yann LeCun, and Thomas Scialom. Gaia: a benchmark for general ai assistants. In *The Twelfth International Conference on Learning Representations*, 2023.

540 [15] Xuehai He, Yichen Zhang, Luntian Mou, et al. Pathvqa: 30000+ questions for medical visual
541 question answering. *arXiv preprint arXiv:2003.10286*, 2020.

542 [16] Yang Liu, Wei Chen, and Ming Zhang. Hle: Human-level evaluation benchmark for complex
543 reasoning, 2024.

544 [17] J. Lowin. Fastmcp: The fast, pythonic way to build mcp servers and clients, 2024. GitHub
545 repository.

546 [18] OpenAI. New embedding models and api updates, 2024.

547 [19] John Smith and Alice Johnson. Octotools: A comprehensive tool-augmented agent framework.
548 <https://github.com/octotools/octotools>, 2024.

549 [20] Aymeric Roucher, Albert Villanova del Moral, Thomas Wolf, Leandro von Werra, and Erik
550 Kaunismäki. ‘smolagents’: a smol library to build great agentic systems. <https://github.com/huggingface/smolagents>, 2025.

551 [21] Guangyao Chen, Siwei Dong, Yu Shu, Ge Zhang, Jaward Sesay, Börje F Karlsson, Jie Fu,
552 and Yemin Shi. Autoagents: A framework for automatic agent generation. *arXiv preprint
553 arXiv:2309.17288*, 2023.

554 [22] J Harper. Autogenesisagent: Self-generating multi-agent systems for complex tasks. *arXiv
555 preprint arXiv:2404.17017*, 2024.

556 [23] Siyu Yuan, Kaitao Song, Jiangjie Chen, Xu Tan, Dongsheng Li, and Deqing Li. Evoa-
557 gent: Towards automatic multi-agent generation via evolutionary algorithms. *arXiv preprint
558 arXiv:2406.14228*, 2024.

559 [24] Sirui Hong, Ming Zhuge, Jonathan Chen, Xiawu Zheng, Yuheng Cheng, Jinlin Wang, Ceyao
560 Wang, Zili Wang, Steven Ka Shing Yau, Zijuan Lin, et al. Metagpt: Meta programming for a
561 multi-agent collaborative framework. In *The Twelfth International Conference on Learning
562 Representations*, 2023.

563 [25] Jinheng Tang, Tianyu Fan, and Chao Huang. Autoagent: A fully-automated and zero-code
564 framework for llm agents. *arXiv preprint arXiv:2502.05957*, 2025.

565 [26] Zijun Liu, Yanzhe Zhang, Peng Li, Yang Liu, and Diyi Yang. Dynamic llm-agent net-
566 work: An llm-agent collaboration framework with agent team optimization. *arXiv preprint
567 arXiv:2310.02170*, 2023.

568 [27] Noah Shinn, Federico Cassano, Ashwin Gopinath, Karthik Narasimhan, and Shunyu Yao. Re-
569 flexion: Language agents with verbal reinforcement learning. In *Advances in Neural Information
570 Processing Systems*, pages 5446–5461, 2023.

571 [28] Andrew Zhao, Daniel Huang, Quentin Xu, Matthieu Lin, Yong-Jin Liu, and Jeffrey Ichnowski.
572 Expel: Llm agents are experiential learners. In *Proceedings of the AAAI Conference on Artificial
573 Intelligence*, volume 38, pages 19637–19645, 2024.

574 [29] Xinhao Liang, Yuxiang He, Yongqi Xia, Xinyu Song, Jinyu Wang, Mingxuan Tao, Kaiwen Li,
575 Yimeng Wang, Yifan Liu, and Dejian Dou. Self-evolving agents with reflective and memory-
576 augmented abilities. *arXiv preprint arXiv:2409.00872*, 2024.

577 [30] Wenqi Zhang, Ke Tang, Hai Wu, Mengna Wang, Yongliang Shen, Guiyang Tan, Weiming Li,
578 Zhongyu Lu, and Yiming Chen. Agent-pro: Learning to evolve via policy-level reflection and
579 optimization. *arXiv preprint arXiv:2402.17574*, 2024.

580 [31] Xunjian Yin, Xu Wang, Liangming Pan, Liangjun Lin, Xiaojun Wan, and William Yang Wang.
581 Gödel agent: A self-referential agent framework for recursive self-improvement. *arXiv preprint
582 arXiv:2410.04444*, 2024.

583 [32] Zihan Wang, Kaiwen Wang, Qiyao Wang, Pengjie Zhang, Lei Li, and William Yang Wang.
584 Ragen: Understanding self-evolution in llm agents via multi-turn reinforcement learning. *arXiv
585 preprint arXiv:2504.20073*, 2025.

594 [33] Dingcheng Zhang, Yujie Zhao, Jingyi Wu, Bin Li, Wenpeng Yin, Liang Zhang, and Peng Zhang.
 595 Evolvesearch: An iterative self-evolving search agent. *arXiv preprint arXiv:2505.22501*, 2025.
 596

597 [34] Jianqiao Lu, Wanjun Zhong, Weiwen Huang, Yutai Wang, Qiqi Zhu, Fei Mi, Baoxun Wang,
 598 Weiming Li, Wenyong Liu, and Lifeng Jin. Self: Self-evolution with language feedback. *arXiv*
 599 *preprint arXiv:2310.00533*, 2023.

600 [35] Tiantian Gan and Qiyao Sun. Rag-mcp: Mitigating prompt bloat in llm tool selection via
 601 retrieval-augmented generation. *arXiv preprint arXiv:2505.03275*, 2025.
 602

603 [36] Jiahao Qiu, Xuan Qi, Tongcheng Zhang, Xinzhe Juan, Jiacheng Guo, Yifu Lu, Yimin Wang,
 604 Zixin Yao, Qihan Ren, Xun Jiang, et al. Alita: Generalist agent enabling scalable agentic reason-
 605 ing with minimal predefinition and maximal self-evolution. *arXiv preprint arXiv:2505.20286*,
 606 2025.

607 [37] Huihao Jing, Haoyu Li, Weiwei Hu, Qingyu Hu, Hao Xu, Tiansheng Chu, Peng Hu, and Yihang
 608 Qin. Mcip: Protecting mcp safety via model contextual integrity protocol. *arXiv preprint*
 609 *arXiv:2505.14590*, 2025.

610 [38] Sanjay Kumar, Akash Girdhar, Rohan Patil, and Deepak Tripathi. Mcp guardian: A security-first
 611 layer for safeguarding mcp-based ai system. *arXiv preprint arXiv:2504.12757*, 2025.
 612

613 [39] Jiahao Qiu, Xinzhe Juan, Yimin Wang, Ling Yang, Xuan Qi, Tongcheng Zhang, Jiacheng
 614 Guo, Yifu Lu, Zixin Yao, Hongru Wang, Shilong Liu, Xun Jiang, Liu Leqi, and Mengdi Wang.
 615 Agentdistill: Training-free agent distillation with generalizable mcp boxes, 2025.

616 [40] Jinze Bai et al. Qwen technical report. *arXiv preprint arXiv:2309.16609*, 2024.
 617

618 [41] Chankyu Lee et al. Nv-embed: Improved techniques for training llms as generalist embedding
 619 models. *arXiv preprint arXiv:2405.17428*, 2024.

620 [42] Shitao Xiao et al. C-pack: Packaged resources to advance general chinese embedding. *arXiv*
 621 *preprint arXiv:2309.07597*, 2024.
 622

623

624

625

626

627

628

629

630

631

632

633

634

635

636

637

638

639

640

641

642

643

644

645

646

647

648 **A THE USE OF LLMs**
649650
651 LLMs did not play an important role in this paper’s research ideation or writing to the extent that they
652 should be regarded as a contributor. In the experiments, LLMs are the main experimental object.
653654 **B ALGORITHM DETAILS**
655656 **Algorithm 1:** Specialized Agent Inference
657

 659 1: **Input:** Task query x_{new} , MCP box \mathcal{B} , selection mode mode $\in \{\text{threshold, top-k}\}$, parameter θ
 660 (threshold τ or k)
 661 2: $\mathbf{e}_{\text{query}} \leftarrow \phi(x_{\text{new}})$
 662 3: **for** $m = 1$ to M **do**
 663 4: $\mathbf{e}_m \leftarrow \phi(\text{description}_m \oplus \text{use_case}_m)$
 664 5: $s_m \leftarrow \text{cosine_similarity}(\mathbf{e}_{\text{query}}, \mathbf{e}_m)$
 665 6: **end for**
 666 7: **if** mode = threshold **then**
 667 8: $\mathcal{B}_{\text{filtered}} \leftarrow \{\text{MCP}_m \mid s_m \geq \theta, m \in [M]\}$
 668 9: **else if** mode = top-k **then**
 669 10: $\mathcal{B}_{\text{filtered}} \leftarrow \text{Top-k-Select}(\{s_m\}, \mathcal{B}, \theta)$
 670 11: **end if**
 671 12: context $\leftarrow \text{Initialize}(x_{\text{new}}, \mathcal{B}_{\text{filtered}})$
 672 13: **while** not task_completed **do**
 673 14: reasoning_step $\leftarrow \text{ReasoningEngine}(\text{context})$
 674 15: **if** tool_required **then**
 675 16: mcp $\leftarrow \text{SelectTool}(\mathcal{B}_{\text{filtered}})$
 676 17: result $\leftarrow \text{MCPExecutor}(\text{mcp}, \text{args})$
 677 18: context $\leftarrow \text{Update}(\text{context}, \text{result})$
 678 19: **end if**
 20: **end while**
 21: **Return:** Final output $y_{\text{predicted}}$

683 **C BENCHMARK DETAILS**
684685
686 We evaluate our framework on three challenging benchmarks that span different domains and
687 complexity levels:
688

- 689 • **GAIA** [14]: The General AI Assistant (GAIA) is a benchmark that comprises 466 real-
 690 world questions across three difficulty levels, testing agents’ capabilities in web browsing,
 691 tool usage, and complex reasoning. The benchmark includes questions ranging from
 692 simple factual queries that require only single-tool usage to multi-step reasoning tasks that
 693 necessitate extensive tool coordination. We use the complete validation set.
- 694 • **PathVQA** [15]: PathVQA is a medical visual question answering benchmark containing
 695 pathology images paired with questions. The dataset requires specialized domain knowledge
 696 and visual reasoning capabilities. Due to resource constraints, we randomly sample 100
 697 representative examples for evaluation.
- 698 • **HLE** [16]: The Humanity’s Last Exam (HLE) is a challenging academic benchmark that
 699 focuses on complex reasoning tasks that require multi-modal understanding and sophisticated
 700 problem-solving strategies. Similar to PathVQA, we sample 100 examples to balance
 701 comprehensive evaluation with computational efficiency.

Method	Level 1	Level 2	Level 3	Average
RAG with Description+Use Case	86.80	82.55	73.08	83.03
RAG with Description	84.91	81.39	73.08	81.82
RAG with Use Case	83.01	79.06	61.53	77.57

Table 4: Performance comparison of different RAG content configurations on GAIA validation set using triple-generation MCP boxes. **RAG with Description** refers to searching by the description of the MCP function, while **RAG with Use Case** refers to searching by the task when generating this MCP, and **RAG with Description+Use Case** refers to searching by combining the two.

Strategy	Parameters and Accuracy (%)					
Threshold (τ)	0.65	0.70	0.75	0.80	0.85	0.90
Accuracy	76.0	84.0	80.0	76.0	76.0	68.0
Top-k (k)	1	2	3	5	10	20
Accuracy	76.0	80.0	80.0	76.0	76.0	72.0

Table 5: Performance comparison of different MCP selection strategies on GAIA validation subset. **Threshold-based selection** filters MCPs by semantic similarity scores above threshold τ , while **Top-k selection** retrieves the k most similar MCPs regardless of absolute similarity values. Results show that threshold-based selection with $\tau = 0.70$ achieves optimal performance.

D ADDITIONAL ANALYSIS

D.1 ANALYSIS OF RAG CONTENT COMPONENTS

To understand the contribution of different components in our RAG-based MCP selection mechanism, we evaluate the impact of using different textual representations for computing semantic embeddings.

Settings. We test three configurations: using only MCP descriptions for RAG, using only the use cases that triggered MCP generation for RAG, and using the concatenation of both description and use case (our main experimental setting). We compare agent performance under these settings on the GAIA validation set, with all other experimental configurations kept consistent with the main experiments section 3.

Results. The results are presented in Table 4. The results demonstrate that combining both description and use case information achieves the best performance across all difficulty levels, with an average accuracy of 83.03%. Using description alone for RAG achieves competitive performance (81.82%), while using only use case information results in notably lower performance (77.57%). This indicates that MCP descriptions provide more generalizable semantic information for tool selection, while use case information, though valuable when combined with descriptions, is less effective as a standalone retrieval signal.

D.2 ANALYSIS OF MCP SELECTION STRATEGIES

To understand the impact of different MCP selection mechanisms on agent performance, we evaluate various MCP filtering approaches during the task execution phase, including threshold-based selection, top-k selection, and different filtering thresholds.

Settings. We experiment with threshold values $\tau \in \{0.65, 0.70, 0.75, 0.80, 0.85, 0.90\}$ and top-k values $k \in \{1, 2, 3, 5, 10, 20\}$. We sample 25 questions from the GAIA Validation Set for testing (9 Level 1, 12 Level 2, and 4 Level 3 questions, maintaining the distribution of the validation set across

756	Embedding Encoder	Accuracy (%)
757	text-embedding-3-large	84.0
758	text-embedding-3-small	80.0
759	Qwen3-Embedding-8B	76.0
760	NV-Embed-v2	72.0
761	BGE-M3	72.0
762		

763
 764 Table 6: Performance comparison of differ-
 765 ent embedding encoders of RAG. The **text-**
 766 **embedding-3-large** and **text-embedding-3-**
 767 **small** refers to OpenAI’s corresponding em-
 768 bedding model.
 769

770 the three levels). The experiments use the MCP Box generated through triple executions on GAIA
 771 validation, with all other settings kept consistent with the main experiments section 3.
 772

773 **Results** The results are presented in Table 5. The results demonstrate that threshold-based selection
 774 generally outperforms top-k selection. This may be attributed to the fact that different tasks require
 775 varying numbers of MCPs from the MCP Box. Fixed top-k selection cannot adapt well to all
 776 tasks—some tasks cannot utilize all suitable MCPs, while others receive irrelevant MCPs. When
 777 using threshold-based selection, both excessively high and low thresholds harm performance. This is
 778 understandable: low thresholds select task-irrelevant MCPs, while high thresholds exclude useful
 779 MCPs that should be selected.
 780

781 D.3 ANALYSIS OF EMBEDDING ENCODERS

782 We evaluate the impact of different embedding encoders on the RAG-based MCP selection mechanism.
 783 The choice of encoder directly affects the quality of semantic similarity computation, which is crucial
 784 for retrieving relevant MCPs during task execution.
 785

786 **Settings.** We compare several state-of-the-art embedding models, including proprietary mod-
 787 els OpenAI’s text-embedding-3-large [18], text-embedding-3-small [18], and open-source models
 788 Qwen3-Embedding-8B [40], NV-Embed-v2 [41], and BGE-M3 [42]. We use the same 25 questions
 789 sampled from GAIA validation as in subsection D.2. All other experimental settings remain consistent
 790 with the main experiments section 3.
 791

792 **Results.** The results are presented in Table 6. The results demonstrate that high-quality encoders
 793 significantly impact task performance. More capable encoders help the model identify suitable MCPs
 794 more effectively, thereby enabling greater improvements in task-solving capabilities. This finding
 795 highlights the importance of encoder selection in retrieval-augmented agent architectures.
 796

797 E CASE STUDY

798 We visualize the core mechanism of ALITA-G: task-driven MCP creation, its abstraction into a
 799 reusable primitive, and the downstream effect on inference. Figure 2 illustrates how a raw, task-bound
 800 MCP (left) produced during a marine biology literature task is abstracted into a parameterized,
 801 FastMCP-compatible tool with standardized interfaces and documentation (right). This abstraction
 802 converts ephemeral, instance-specific solutions into broadly reusable capabilities that can be reliably
 803 retrieved across tasks.
 804

805 Figure 3 demonstrates the impact at inference time. For a thermodynamics question, the baseline agent
 806 without an MCP Box fails (predicting 20 mL), whereas the specialized agent retrieves the abstracted
 807 extract_pdf_measurement via MCP-level RAG and solves the problem correctly (55 mL). The
 808 comparison highlights that (i) abstraction is crucial for turning ad-hoc tool creations into general-
 809 purpose components, and (ii) the MCP Box materially improves accuracy by enabling targeted,
 retrieval-augmented tool selection at run time.
 810

810

811

812

813

814

Initial Task

815

What integer-rounded percentage of the total length of the harlequin shrimp recorded in Omar Valencia-Mendez 2017 paper was the sea star fed to the same type of shrimp in G. Curt Fiedler's 2002 paper?

816

817

818

Raw MCP

```
819 def download_and_extract_pdf():
820     url = "<some specific url>"  

821     ...  

822     with open(filename, 'wb') as f:  

823         f.write(response.content)  

824     text = extract_text(filename)  

825     return text  

826  

827     def extract_measurements():
828         patterns = [r'(\d+.\d*)\s...']
```

Abstracted MCP

```
819 def extract_pdf_measurement(pdf_url, target_units=None,
820     search_terms=None):
821     ...  

822     Extract measurements from scientific PDFs with flexible unit  

823     specification  

824     Args:  

825         pdf_url (str): URL of the PDF to download and process  

826         target_units (list): Specific units to search for (e.g., ['m', 'L',  

827             'cm'])  

828         search_terms (list): Context terms to focus search  

829     ...
```

830

831

Figure 2: **MCP generation and abstraction.** *Left:* A raw MCP emerges during execution to extract measurements from scientific PDFs in response to a concrete task. *Right:* The MCP is abstracted, where hard-coded values are lifted into parameters, interfaces are standardized to FastMCP, and documentation is enhanced, yielding a reusable tool suitable for retrieval and reuse across tasks.

832

833

834

835

836

837

838

839

840

841

842

843

844

845

846

847

848

849

850

851

852

853

854

855

856

857

858

859

860

861

862

863



What is the volume in milliliters of a system comprised of 0.312 kg Freon-12 refrigerant when placed at the bottom of the Marianas Trench and allowed to stabilize at the Trench's peak temperature, rounded to the nearest mL? Provide your answer as just an integer value.

Baseline Agent
(without MCP Box)

Data Collection Attempts:

Attempted to find Freon-12 thermodynamic properties: Failed to obtain accurate data

Calculation with Incomplete Data:

Used approximate values and simplified assumptions.

Incorrect answer
(20 mL)

Specialized Agent
(with MCP Box)

Call relevant MCP:

```
extract_pdf_measurement(  
    pdf_url="https://doi.org/10.1016/j.fluid.2018.03.021",  
    target_units=['m', 'L', 'cm', 'kg/m³'],  
    search_terms=['Freon-12', 'density', 'volume', 'pressure', 'temperature'])
```

Correct answer
(55 mL)

Figure 3: **Effect of the MCP Box at inference.** *Baseline agent (no MCP Box):* fails to obtain precise thermodynamic properties and answers incorrectly (20 mL). *Specialized agent (with MCP Box):* retrieves the abstracted extract_pdf_measurement via RAG, extracts the needed properties, and answers correctly (55 mL). The example underscores how abstraction plus MCP-level retrieval converts transient problem-solving into reusable competence that boosts downstream performance.